# Multiwavelength analysis of the Young Open Cluster NGC 2362

A. J. Delgado, O. González-Martín, E.J. Alfaro
Instituto de Astrofísica de Andalucía, CSIC, Apdo 3004, 18080-Granada, Spain

and

J. Lin Yun
Observatório Astronómico de Lisboa, Tapada da Ajuda 1349-018 Lisboa, Portugal

## ABSTRACT

We present a multiwavelength analysis of the young open cluster NGC 2362. $UBVR_CI_C$ CCD photometric observations, together with available data in the *Chandra* data base, near infrared data from the Two Micron All Sky Survey (2MASS), and recently published H$\alpha$ spectroscopy were used to get information about the evolutionary stage of the cluster and the main physical properties of its stellar content. Cluster membership is estimated for every individual star by means of ZAMS and isochrone fitting. The cluster is confirmed to host a richly populated pre-main sequence (PMS), and to contain a large amount of X-ray emitting stars, which reach from the PMS members of GK spectral type, up to the most luminous OB type main sequence (MS) members. The PMS cluster members show no significant age spread, and the comparison to both PMS and post-MS isochrones suggests a younger age for the more massive MS than for lower mass PMS members. The analysis allows to asses the validity of currently used pre-main sequence evolutionary models, and supports the suggestion of a well defined positive correlation of the X-ray emission from PMS stars with their bolometric luminosity. Clear differences are found on the other hand, between the X-ray activity properties of MS and PMS cluster members, both in the relation between X-ray luminosity and bolometric luminosity, and in spectral properties as well.

*Subject headings:* open clusters and associations: individual: NGC 2362 — stars: pre-main sequence

## 1. Introduction

The young open cluster NGC 2362 has been the subject of recent attention from several authors, as an adequate object for the study of the star formation processes (Moitinho et al 2001, Haisch et al. 2001, Dahm 2005, D05 in the following). Located in the third galactic quadrant, it is

little affected by reddening and, despite its youth, shows a relative absence of intracluster material (Balona & Laney 1996). All this allows the observation of its stellar population in a wide range of masses, moving from the low mass PMS stars to massive OB stars populating the upper part of the color-magnitude diagram (CMD)

The photometric observations of NGC 2362 were carried out in the framework of a current project devoted to detect and study pre-main sequence (PMS) stars among the members of young open clusters. This project is based on optical $UBVRI$, and eventually H$\alpha$ observations of galactic clusters, inside the age range between 1 and 10 Myr, and located at distances from the Sun not farther than 3-4 kpc. These constraints should leave objects with observable PMS members of spectral types from A to K, detectable in photometric diagrams deep dwon to $V$ 21-22, depending on reddening. These observations are feasible with small telescopes, and can be obtained for a wide sample of clusters in the Cygnus and Perseus galactic spiral arms, as well as for some clusters located at larger distances in the direction of the galactic anticenter. A presentation of the results obtained up to now in this project will be the subject of another paper.

On the other hand, the investigation of X-ray emission from PMS stars received increasing attention in recent years after the new space missions, able to provide measurements of high spectral and spatial resolution. As a consequence, the debate about the physical mechanisms that originate this activity has gained in richness and insight (see Preibisch et al. 2005, and references there in).

In this paper we collect $UBVR_CI_C$ CCD photometry of our own, X-ray data on sources detected in the field by the *Chandra* Advanced CCD Imaging Spectrometer (ACIS)[1], $JHK$ photometry from the 2MASS[2] data base, and H$\alpha$ emission and Li absorption from PMS cluster members (D05), in order to analyze the evolutionary stage of the cluster members ant its connection with the X-ray activity.

## 2. The data

The optical observations were secured during two nights in December 2000, at the CTIO observatory with the YALO 1m telescope[3]. As mentioned above, these observations are included in a long term search for PMS stars in young open clusters. A thorough presentation of the southern clusters observed in this program, including the detailed description of the reduction and calibration procedures, will be the subject of a forthcoming paper. This publication will also include the photometric catalogue of all objects observed.

---

[1] `http://cxc.harvard.edu/cda/`

[2] `http://www.ipac.caltech.edu/2mass/`

[3] YALO is the **Y**ale-**A**URA-**L**isbon-**O**hio consortium (Bailyn et al. 1999)

The pixel coordinates of our catalogue were transformed to equatorial coordinates using the IRAF[4] tasks `ccmap` and `xy2rd`. The matching provides $UBVR_CI_CJHK$ photometry for 725 stars. Among them, 551 have Photometric Quality flag A to D in all three $JHK$ bands (see the catalogue description at `http://www.ipac.caltech.edu/2mass/releases/allsky/doc/`).

Data from *Chandra*-ACIS in the field of NGC 2362 have been retrieved from the public data archive. NGC 2362 was observed with *Chandra X-Ray Observatory* on UT date 2003 December (Obs. ID 4469). These data have been recently reported by Damiani et al. (2005). The dataset was filtered using the lightcurve in the 0.5 to 8 keV band ACIS-S CCD. The CIAO LC_CLEAN tool was used to remove flare periods. The total exposure time, after removing periods containing flares, is 92.7 ks. The CIAO CELLDETECT source detection routine was then used on the level 2 event data to produce a list of point sources. Cell sizes between 4 pixels and 8 pixels were used. We have detected 231 X-ray point sources in the ACIS CCD in the range between 0.5 to 8.0 keV band.

The ACIS field of view in these observations covers 56% of the field in our UBVR$_C$I$_C$ observations. Matching with the 2MASS coordinates results in the identification of optical counterparts for 152 sources. Of these, 127 fall in the region of the $V$, $(B-V)$ and $(V-I)$ color-magnitude diagrams occupied by the cluster members.

Finally, a recently published photometric and spectroscopic study of the cluster (D05), includes equivalent widths of H$\alpha$ in emission for 99 stars in common with our photometric catalogue, 69 of them also with measured equivalent width in the absorption line LiI 6708Å.

In the following we consider in our analysis those stars selected as members on the basis of our optical photometry (see below), and with values in at least one of the data bases used.

## 3. Analysis

### 3.1. Optical Photometry

Distance, color excess and membership to the cluster are determined with the procedure designed by Delgado et al. (1998). Briefly, using the ZAMS line (Schmidt-Kaler 1982) we calculate values of color excess $E(B-V)$, visual absorption A$_V$=3.1$\times E(B-V)$, and absolute magnitude M$_V$ for all possible main sequence (MS) cluster members. A plot of $V$-A$_V$ versus M$_V$, allows to establish membership of evolved and unevolved MS members, and discard possible non members. 30 stars are selected in total as MS members. The mean values of color excess and distance modulus for the unevolved members are then used as reference values to analyse membership of

[4]The Image Reduction and Analysis Facility (IRAF) is distributed by the national Optical Astronomical Observatory, which is operated by the Association of Universities for Research in Astronomy, Inc. (AURA) under cooperative agreement with the National Science Foundation

the remaining stars. These amount to $E(B-V) = 0.12 \pm 0.04$, $V_0 - M_V = 10.78 \pm 0.15$. The quoted errors are the rms deviations of the mean.

In this process, we compute for every star several values of the color excess and distance modulus by ZAMS fitting, and also the values given by comparison to theoretical PMS isochrones. In absence of phenomenological reference lines for PMS stars, of the type of observational ZAMS, PMS isochrones are used to assign probable membership to every star. A star is considered as member when color excess and distance, in respect to the isochrone, coincide inside the errors with the above referred reference values, in at least two CM diagrams.

In this calculation we use three sets of PMS isochrones by D'Antona & Mazzitelli (1997), Palla & Stahler (1999), and Siess, Dufour & Forestini (2000) (respectively referred to in the following as D97, P99, S00) for ages between 1 and 10 million years. The theoretical isochrones by D97 and P99 are transformed to the observational CM diagrams with the calibrations by Kenyon & Hartmann (1995). A total of 276 stars are selected as PMS cluster members, in respect to at least one of the three isochrone sets used.

Because of the larger photometric errors for fainter stars, most of the PMS candidates are selected as members with respect to several isochrones. The average value of their ages provides a formal age for every assigned PMS member star, and the median of all members is adopted as the age of the PMS cluster sequence. The resulting ages for the three sets of isochrones amount to 4.3±2.6, 6.0±2.4, and 5.9±2.1 Myr for D97, P99, and S00 isochrones respectively. These values indicate coincidence of ages within the uncertainties and little age spread among PMS cluster members. On the other hand, the comparison to post-MS isochrones from the Padova group (Girardi et al. 2002) as plotted in Figure 1, suggests an upper limit of 4 Myr for the most massive MS cluster members.

The plot in Figure 1 shows post-MS isochrones for 4 and 10 Myr (Padova), and PMS isochrones for 1, and 10 Myr (D97, P99, S00) in the $V,(V-I)$ CM diagram. The stars classifed as members by any one of the fittings described above are marked with larger dots, while those found to be optical counterparts of detected X-ray sources, as well as those in common with the H$\alpha$ study by D05 are marked with crosses and squares, respectively. We remark that 85% of the detected X-ray sources, with optical counterpart in the appropiate range of color and magnitudes are selected as members by our procedure, and 66 out of 80 stars with H$\alpha$ emission in the overlapping field and adequate magnitude range turn out to be assigned PMS members (in particular, 50 out of the 58 stars with both X ray detection and Ha emission). The good agreement between these independent criteria of both PMS nature of the stars, and membership to the cluster shows the reliability of the membership estimate by the isochrone fitting used – by similarity to the ZAMS fitting procedure commonly used to estimate distances for MS stars.

The relation of ages determined from PMS and Post-MS isochrones, as well as the possible age spread among PMS cluster members, are adressed in almost every investigation dealing with PMS stars in young clusters, and the evidences are not conclusive in either sense. In our case,

as explained above, no significant age spread is found among PMS cluster members, although different values are found from comparison to different PMS models. We remark again the comparatively younger ages determined from the D97 isochrones, and most interestingly, the lower age obtained for upper MS stars than the one inferred for PMS cluster members. These kind of trend has been found, for instance, in the association Sco-Cen OB2 by Mamajek, Meyer & Liebert (2002), and would suggest later formation of most massive stars.

### 3.2. Chandra-ACIS data

The computation of X-ray luminosity from count rates for the detected sources proceeds after the selection of the best temperature model using diagrams of hardness ratios.

We compute the ratios HRA=($C_2$-$C_1$)/($C_2$+$C_1$) and HRB=($C_3$-$C_2$)/($C_3$+$C_2$), where $C_1$, $C_2$, and $C_3$ are the total counts in the bands 0.6-1.6 keV, 1.6-2.0 keV, and 2.0-8.0 keV, respectively. The values for our sources are compared in the HRB vs HRA diagram to a single temperature grid (Raymond-Smith) calculated with the *Portable Interactive Multi-Mission Simulator* (PIMMS). This plot is shown in Figure 2. In the range beween 0.4 and 4 keV, the temperature model that best reproduces the distribution of our sources corresponds to kT=1.7 keV, with an Hydrogen column density of $2.5 \times 10^{21}$ cm$^{-2}$, consistent with the $N_H$ value from the HI map (see `http://heasarc.gsfc.nasa.gov/cgi-bin/Tools/w3nh/w3nh.pl`). With these parameters, fluxes are calculated for each source in the ranges 0.5-2.0 keV, 2.0-8.0 keV, and the total flux in the range 0.5-8.0 keV. To compare with the results obtained by assigning different temperature models to PMS and MS stars, we have also calculated the fluxes in the same ranges for temperatures of 2.16 keV and 0.6 keV for PMS and MS stars, respectively (Flaccomio, Micela & Sciortino 2003).

In Table 1 we list the data for those stars in our photometric catalogue, which are also detected in X-rays, or included in the D05 publication. The table lists the identification number, and membership identification in columns 1 and 2: MS and PMS members are respectively denoted with 1 an 2 in column 2. Equatorial coordinates (Equinox 2000) in columns 3,4. Color indices $V$, $(U-B)$, $(B-V)$, $(V-R)$, and $(V-I)$ in columns 5 to 9, $(H-K)$ increment with respect to the reddenning line in the $(J-H),(H-K)$ diagram in column 10. Equivalent widths from D05 in H$\alpha$ and LiI 6708Å, in columns 11, 12. Calculated X-ray fluxes (ergs/sec.cm$^2$) in the bands 0.6-2.0 keV, and 2.0-8.0 keV, in columns 11 and 12. And X-ray luminosity (calculated as the decimal logarithm of the total intrinsic flux), and Bolometric Luminosity, in columns 12 and 13. The color excesses and slope of the reddening line in the $(J-H),(H-K)$ diagram follow the reddening law from Cardelli, Clayton & Mathis (1989). The intrinc total flux is calculated with the distance obtained from our optical photometry. The contents of Table 1 is accesible in electronic format.

The first evidence that stands out in the observations is the wide range of colors and magnitudes covered by the detected X-ray sources, in particular the considerable amount of MS

stars showing this activity, as compared to other clusters of similar characteristics, as NGC 6530 (Prisinzano et al. 2005). The deeper and more exhaustive observations of Orion, described by Stelzer et al. (2005), also show a generalized presence of X-ray activity among OB type stars. The authors suggest a classification in two different types of mechanism for the X-ray activity in their OB-type MS stars. Following this, the X-ray activity detected from OB stars in NGC 2362 could be mainly adscribed to binary companions, rather than to the presence of strong winds (Stelzer et al. 2005). We note however that some of these member stars show signs of NIR excess in the $(J-H),(H-K)$ diagram (separation from the reddening line larger than their error bar. See Table 1). This could be interpreted as a consequence of a certain amount of circumstellar material around these stars, which could be still in the PMS stage.

Clear differences can be observed otherwise between the properties of X-ray activity in MS and PMS cluster members. Figure 3 shows a plot of $\log L_X$ vs $\log L_{Bol}$. $L_{Bol}$ is calculated with the bolometric corrections from the calibration by Kenyon & Hartmann (1995). The figure shows the different behaviour of PMS and MS members, represented respectively as dots and crosses. We observe that both PMS ans MS stars cover the same range in $L_X$. On the other hand, there is a clear correlation between both luminosities for PMS stars up to spectral type F ($\log L_{Bol} \simeq 34.4$), which vanishes for earlier type PMS candidate members and for MS stars. This different behaviour has been found as a characteristic feature in PMS versus MS stars (Preibisch et al. 2005). We note that most PMS members fall into the category of so called WTTs (weak line T-Tauri stars), as it has been shown by the H$\alpha$ analysis of D05. In particular, only 7 stars in our sample, have equivalent width of H$\alpha$ in emission larger than 10 Å, usually adopted as the separating value between CTTs and WTTs (D05).

Te spectral characteristics of both subsamples also show a different beaviour. In Figure 4 we plot the ratio between hard (2-8 keV) and soft (0.5-2 keV) fluxes, as listed in Table 1. A softening of the X-ray emission is observed for PMS star as $L_{Bol}$ increases. This trend again seems to dissapear for the MS and for the earliest type PMS candidate members. As referred above, the same spectral model has been used to compute fluxes for both PMS and MS members, corresponding to a plasma at temperature of 1.6 keV. Some authors distinguish between both evolutive stages, assigning harder spectra to PMS stars than to those in the main sequence, (Flaccomio, Micela & Sciortino 2003). We wish to stress that the tendency shown in Figure 4 is also apparent, and even enhanced, if we compute hard and soft fluxes with different models of 2.16 keV and 0.6 keV, respectively for PMS and MS stars. The softening of X-ray activity for MS stars, even massive stars, as compared to PMS stars has also been established in recent works (Preibisch et al. 2005, Stelzer et al. 2005).

As mentioned above we wish to specifically point out the behaviour of the PMS candidate members of the earliest spectral type in the cluster (around AF). Although they are PMS candidates according to the optical photometry, and the comparison to PMS isochrones, their X-ray activity show features closer to those from MS stars, both in the relation of $L_X$ to $L_{Bol}$, and in the hehaviour of their hardness ratio as well.

Finally, from the analysis of several star forming regions in a wide range of ages, Flaccomio et al. (2003) have concluded thax X-ray activity increases with age, as the envelopes and disks of stars progressively dissapear. Also Stassun et al. (2004) state that the emission of X-rays can be obscured or modulated by accretion processes, but these are not the origin of the X-ray activity.

This behaviour of the X-ray activity with age is not apparent in a sample where all stars belong to a cluster or association, and much less in a case like NGC2362, where the age spread is small or even absent. However, the joint evidence from our data sources allow some check of this age effect, which can be called more properly evolutionary effect. For 36 stars in our sample, there are both X ray emission, and equivalent widths of the absorption LiI 6708Å (D05), commonly considered as a sign of PMS nature (Bertout 1989). The strength of this absorption (WLi) should be smaller for PMS stars closer to the main sequence (Martín 1997, Palla et al. 2005). When all stars can be considered to have the same age, a variation of WLi can still be expected simply because stars of different masses will have reached different PMS evolutionary stages in the same evolving time. Considering this, we can check the dependence of $L_X$ with Wli, as an indicator of evolutionary status in the PMS phase. We simply compute a linear fit of $\log L_X$ vs $(V - I)$, and plot the residuals versus WLi. The plot is shown in Figure 5, together with a median fit. The lack of a trend in this plot, and even the marginal indication of an increase of $L_X$ with WLi, confirms the absence of age spread among PMS cluster members. On the other hand, this marginal increase seems to indicate a tendency opposite to the general trend shown by stars in a wide range of ages (Flaccomio et al. 2003). That is, X-ray activity is stronger for older stars. The tendency shown in the present data allows little more than a speculation, but if real it could be reproducing the last phase of the time evolution of X-ray activity from the PMS to the MS phase. In this phase, the possible disk vanishing process and decrease of accretion activity are no longer present, and the evolution of X-ray emission would be entirely reflecting changes that take place in the stars interior.

## 4. Conclusions

The joint evidences discussed above lead to the following conclusions. The isochrone fitting to establish PMS membership for individual stars provides reliable results. This follows from the agreement between membership asignements using isochrone fitting, and the signs of PMS nature deduced from observed properties of the stars, such as X-ray activity and presence of specific spectral features, namely H$\alpha$ emission and LiI 6708Åabsorption.

The age estimates from the three sets of PMS isochrones used provide values wich range from 4 to 6 Myr, with the models by D'Antona & Mazzitelli (1997), Siess, Dufour & Forestini (2000), and Palla & Stahler (1999). This difference can be considered as an indication of little, if any, age spread among the PMS cluster members. The comparison of the upper CM diagram with post MS isochrones from Girardi et al. (2002), indicates an upper limit for the MS cluster member of 4 Myr. This result seems to suggest that the most massive stars were formed later, when the low

mass tail was already in the PMS evolutionary stage.

A large number of B-type MS cluster members, as compared with the findings in a cluster of similar properties as NGC 6530 (Prisinzano et al. 2005), are found to be optical counterparts of detected X-ray sources. A clearly distinct behaviour is observed in the properties of the X-ray activity from PMS and MS stars. Those show a well correlated increase with of $L_X$ with $L_{Bol}$, and a decreasing hardness ratio, calculated as the ratio of fluxes above and below 2 keV. The MS stars show values of $L_X$ in the same range covered by the PMS stars, but do not show any correlation between both luminosities, and the suggested variation of hardness ratio with luminosity is also absent, whereby this parameter takes lower values than it does for PMS stars. These results agree with the findings and general properties of X ray activity in PMS stars, obtained from the analysis of closer star forming regions (Flaccomio et al. 2003, Preibisch et al. 2005, Stelzer et al. 2005).

This work has been supported by the spanish MCYT through grants AYA2004-05395, and AYA2003-0128. OGM acknowledges the financiation from MCYT through grant FPI BES-2004-5044. This publication makes use of data products from the Two Micron All Sky Survey, which is a joint project of the University of Massachusetts and the Infrared Processing and Analysis Center/California Institute of Technology, funded by the National Aeronautics and Space Administration and the National Science Foundation. The work has also made use of the BDA Open Clusters Data Base, designed and maintained by J.C. Mermilliod, at the Geneva Observatory, and of of the NASA ADS Abstract Service.

## REFERENCES

Balona L.A., and Laney C.D. 1996, MNRAS, 281, 1341

Bailyn, C., DePoy, D., Agostinho, R., Mendez, R., Espinoza, J., and Gonzalez, D. 1999, The First Year of Operations of the YALO Consortium, AAS 195, 8706

Bertout, C. 1989, ARA&A, 27, 351

Cardelli, J.A., Clayton, G.C., and Mathis, J.S. 1989, ApJ, 345, 245

Dahm S.E. 2005, AJ, 130, 1805 (D05)

Damiani, F., Micela, G., Sciortino, S., Huélamo, N., Harnden, F.R., and Murray, S. 2005, in "Star Formation in the Era of Three Great Observatories". Cambridge, MA, July 2005. `http://cxc.harvard.edu/stars05/agenda/program.html`, p. 33

D'Antona, F., and Mazzitelli, I. 1997 , 'Evolution of low mass stars' in "Cool stars in Clusters and Associations", eds. G. Micela and R. Pallavicini, Mem. S.A.It., 68, 807

Delgado, A.J., Alfaro, E.J., Moitinho, A., and Franco, J. 1998, AJ, 116, 1801

Flaccomio, E., Micela, G, and Sciortino, S. 2003, A&A, 402, 277

Girardi, L., Bertelli, G., Bressan, A., Chiosi, C., Groenewegen, M.A.T., Marigo, P., Salasnich, B., and Weiss, A. 2002, A&A, 391, 195

Haisch, K.E. Jr., Lada, E.A., Lada, C.J. 2001, ApJ, 553, 153

Kenyon, S.J., and Hartmann, L. 2005, ApJS, 101, 117

Mamajek, E.E., Meyer, M.R., and, Liebert, J. 2002, AJ, 124, 1670

Martín, E.L. 1997, A&A, 321, 492

Moitinho, A., Alves, J., Huélamo, N., Lada, C.J. 2001, ApJ, 563, L73

Palla, F., Randich, S., Flaccomio, E., and Pallavicini, R. 2005, ApJ, 626, L49

Palla, F., and Stahler, S.W. 1999, ApJ, 525, 772

Preibisch, T., Yong-Cheol, K., Favata, F., Feigelson, E.D., Flaccomio, E., Getman, K., Micela, G., Sciortino, S., Stassun, K., Stelzer, B., and Zinnecker, H. 2005, ApJS160, 401

Prisinzano, L., Damiani, F., Micela, G., and Sciortino, S. 2005, A&A, 430, 941

Schmidt-Kaler, T. 1982, in *Astronomy & Astrophysics*, Landolt-Börnstein. Numerical Data & Functional Relationships in Science & Technology. Group VI, Vol 2b, p. 14ff. Eds. K. Schaifers & H.H. Voigt (Springer Verlag, Berlin)

Siess, L., Dufour, E., and Forestini, M. 2000, A&A, 358, 593

Stassun, K.G., Ardila, D.R., Barsony, M., Basri, G., and Mathieu, R.D. 2004, AJ, 127, 3537

Stelzer, B., Flaccomio, E., Montmerle, T., Micela, G., Sciortino, S., Favata, F., Preibisch, T., and Feigelson, E.D. 2005, ApJS, 160, 557

Fig. 1.— $V, (V - I)$ Color-Magnitude diagram for NGC 2362. The post-MS isochrones for 4 and 10 Myr, and PMS isochrones for 1 an 10 Myr from the three model sets used, are shown. Larger dots are photometric cluster members. Crosses denote X-ray detected stars, and squares, stars included in the H$\alpha$ catalogue by Dahm (2005)

Fig. 2.— Plot of ratio HRB versus HRA (see text). The grid plotted was calculated for a Raymond-Smith model, within the ranges of temperature (keV) and logaritmus of column density ($cm^{-2}$) indicated by the labels. Triangles: PMS stars; small black stars: MS stars; big black star: mean value of all the data. Only stars with count number above 10 in the range 4.5-8 keV are used, to reduce the error of the comparison.

Fig. 3.— Plot of the X-ray luminosity, $L_X$ versus bolometric luminosity, $L_{Bol}$, for the members stars with detected X-ray activity. Crosses denote the stars selected as MS members, and dots the stars selected as PMS members.

Fig. 4.— Hardness ratio, defined as the quotient of the hard to soft fluxes listed in Table 1, is plotted versus bolometric luminosity for the member stars with detected X-ray activity. The symbols have the same meaning as in Figure 2.

Fig. 5.— Plot for the member stars with both X-ray activity detected in the ACIS data, and equivalent width of Li6708 (Wli) from the work of Dahm (2005). The residuals of the linear fit of $L_X$ vs $(V - I)$, $L_X$=31.09-0.61*$(V - I)$ (see text), are plotted versus WLi. A median fit is also plotted, that shows a slight positive correlation

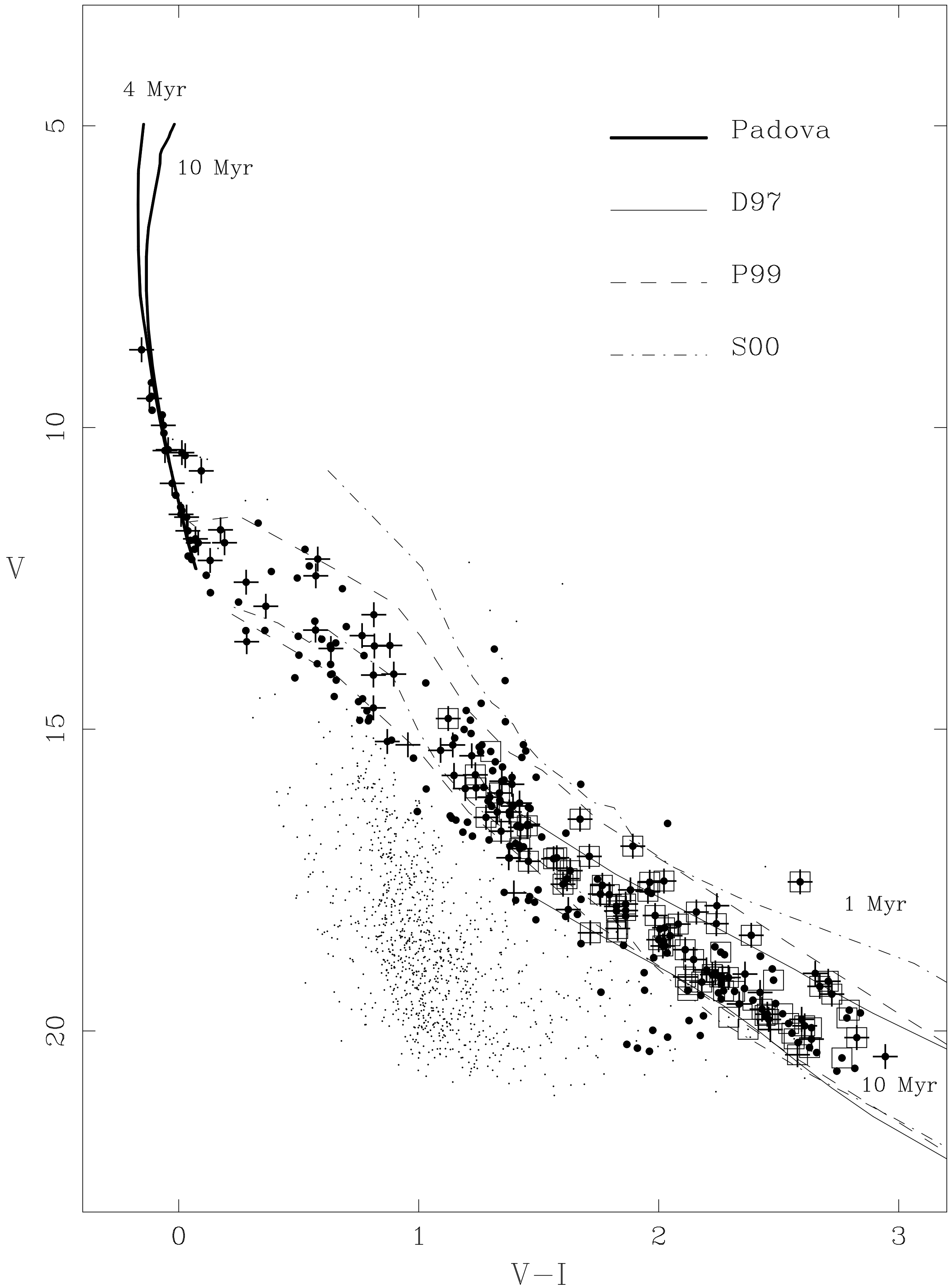
4 Myr
10 Myr
Padova
D97
P99
S00
1 Myr
10 Myr
V
V−I
5
10
15
20
0
1
2
3

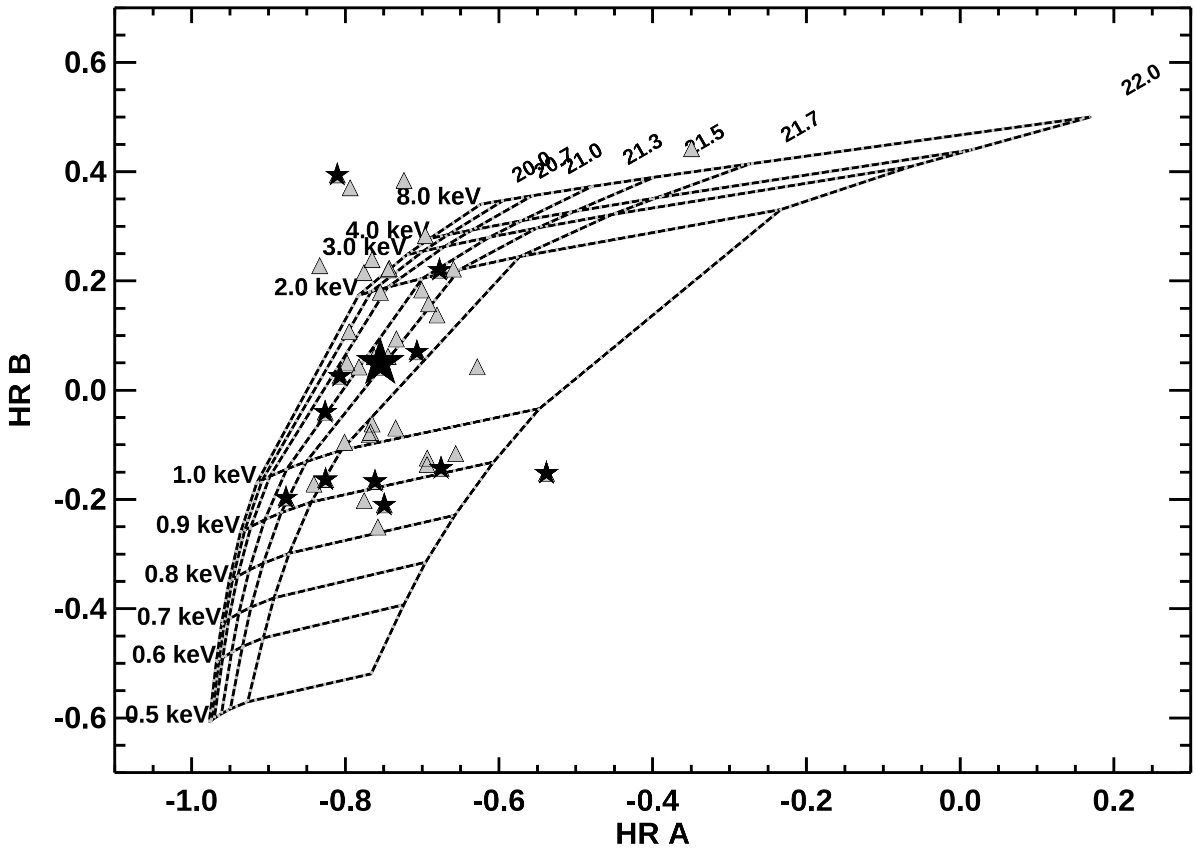

HR B
HR A
0.6
0.4
0.2
0.0
-0.2
-0.4
-0.6
-1.0
-0.8
-0.6
-0.4
-0.2
0.0
0.2
8.0 keV
4.0 keV
3.0 keV
2.0 keV
1.0 keV
0.9 keV
0.8 keV
0.7 keV
0.6 keV
0.5 keV
20.0
20.7
21.0
21.3
21.5
21.7
22.0

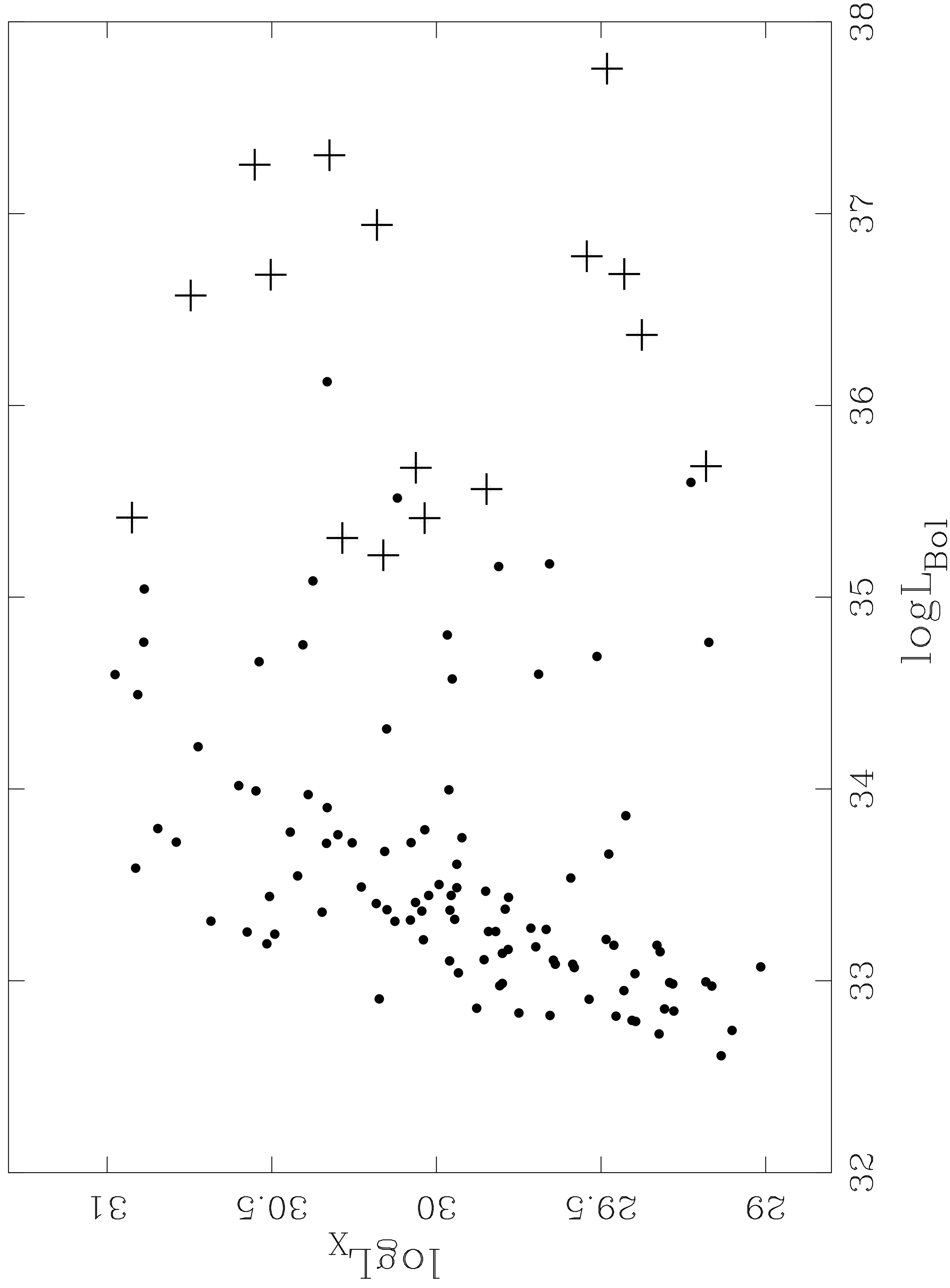
log L_Bol
log L_X
32
33
34
35
36
37
38
29
29.5
30
30.5
31

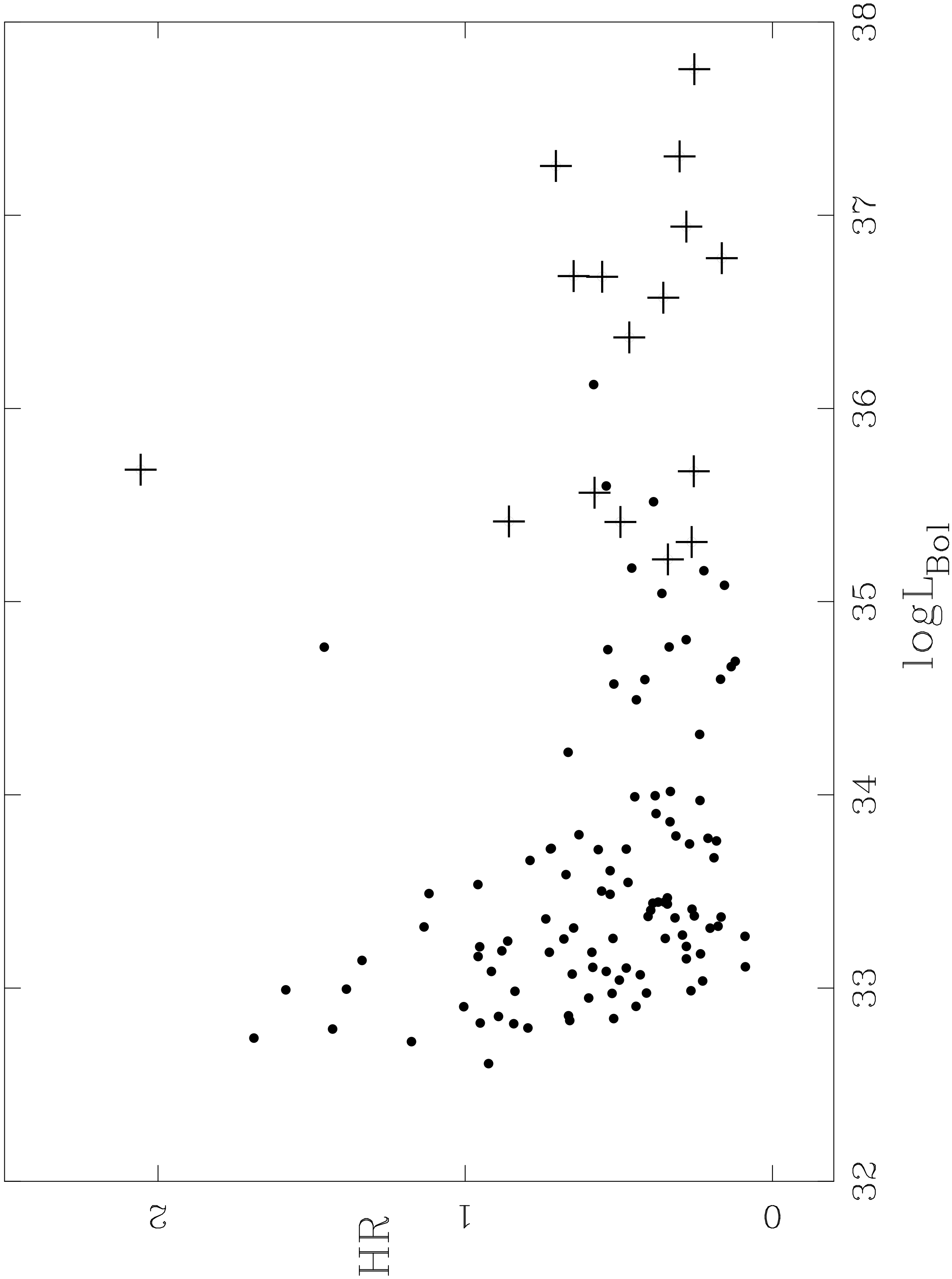

HR
0
1
2
log L$_{Bol}$
32
33
34
35
36
37
38

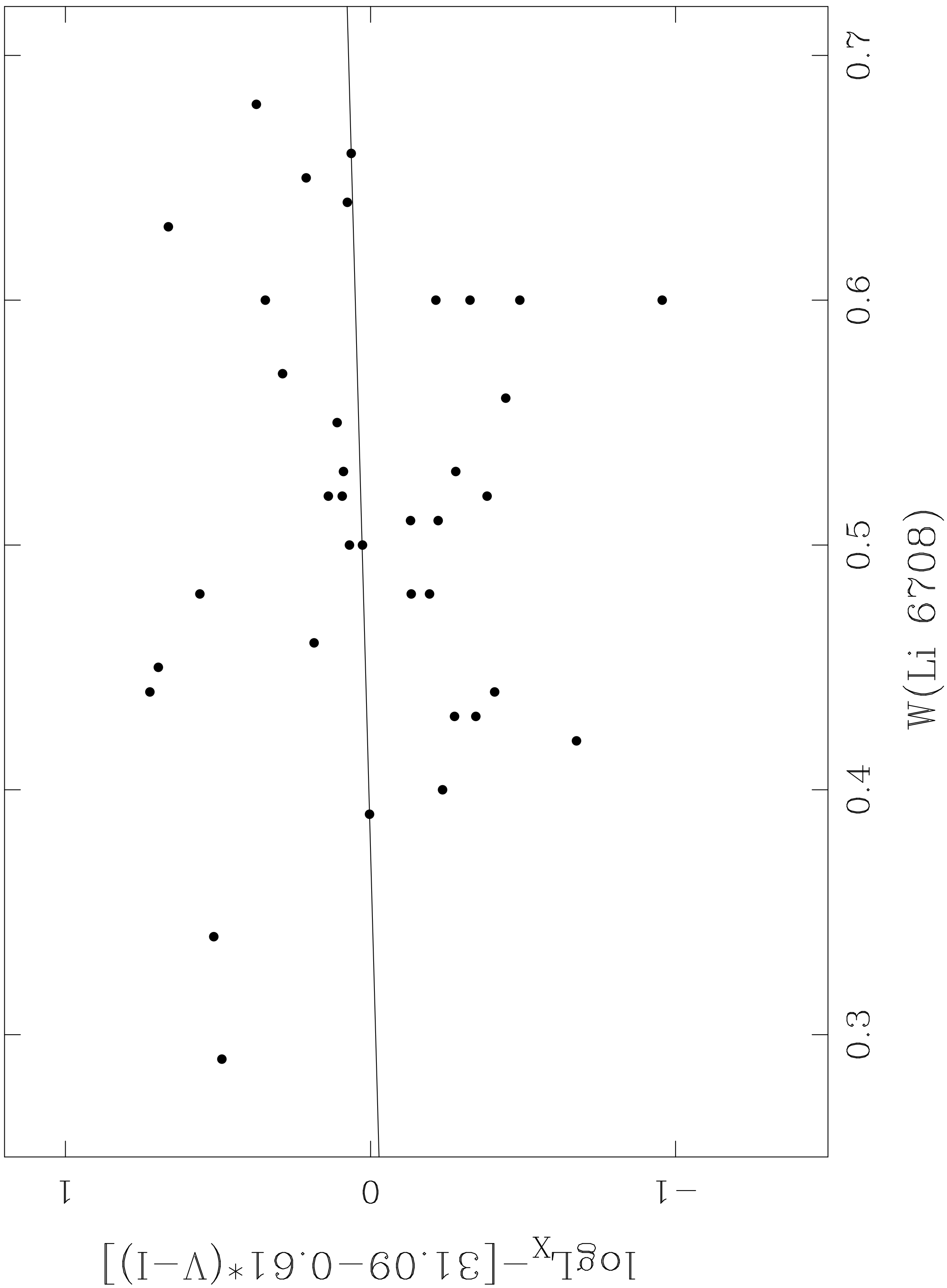
0.3
0.4
0.5
0.6
0.7
W(Li 6708)
1
0
−1
logL$_X$−[31.09−0.61*(V−I)]